International Journal of Ocean System Engineering 2(2) (2012) 97-105
http://dx.doi.org/10.5574/IJOSE.2012.2.2.097

Development of Design Static Property Analysis of Mooring System Caisson for Offshore Floating Wind Turbine

Asgar Ahadpour Dodaran[1] and Sang Kil Park[1*]

[1] *Department of Civil Engineering, Pusan National University, Busan, Korea*

(Manuscript Received February 18, 2012; Revised March 5, 2012; Accepted May 25, 2012)

Abstract

A all floating structures operating within a limited area require, stationkeeping to maintain the motions of the floating structure within permissible limits. In this study, methods for selecting and optimizing the mooring system Caisson for floating wind turbines in shallow water are investigated. The design of the mooring system is checked against the governing rules and standards. Adequately verifying the design of floating structures requires both numerical simulations and model testing, the combination of which is referred to as the hybrid method of design verification. The challenge in directly scaling moorings for model tests is the depth and spatial limitations of wave basins. It is therefore important to design and build equivalent mooring systems to ensure accurate static properties (global restoring forces and global stiffness).

Keywords: Floating Structure, Caisson, Mooring System, Static Properties.

1. Introduction

With the increasing demand for energy and the limited oil and gas deposits, focus is being directed toward renewable energy sources. Wind energy, as one of these renewable energy sources, has been utilized for agricultural purposes for centuries, and also became important for power production in the second half of the 20th century. With the goal of taking advantage of the enormous wind power potential offshore, several participants in the international energy business have installed and commercialized interconnected bottom-fixed wind turbine structures in areas of shallow water. However, the water depth strongly limits the extent of such applications, because the support structures of offshore wind turbines become highly dynamic, having to cope with combined wind and hydrodynamic loading in addition to the complex dynamic behavior of the wind turbine itself. Wind turbines installed on floating substructures are therefore proposed in order to utilize the potential for harvesting wind energy in areas where bottom-fixed structures are not feasible. The development and possible commercializing of floating offshore wind turbines are presently being investigated by several developers, technology providers, and research institutes worldwide. The spar concept is one design that has been proposed as a substructure for floating offshore wind turbines.

The constant demand for offshore resources has moved the industry into an era of increasing applications of deep water technology and concepts for better engineering productivity. The sustained drive to improve the harvests from offshore oil exploration, production, and transportation has led to the existence of various structures, designed to meet the specific needs of the industry under specific circumstances. In ocean depths widely defined as deep water (500m up to 3000m), floating structures find the most use in offshore operations because the construction and performance of fixed structures for such depths would be enormously expensive, and carry very high engineering risks. Floating offshore vessels, require stability to be operational, especial-

*Corresponding author. Tel.: +82-51-510-2427, Fax.: +82-51-513-9596
E-mail address: sakpark@pusan.ac.kr

ly under extreme environmental conditions. Mooring systems are therefore required to provide such stability against vessel dynamics, while ensuring allowable excursions. With so much depending on the mooring systems of these floating structures, it is essential to understand, with a high degree of accuracy, the performance of each of the system components and the global response of the mooring system. The performance of any mooring system is typically a function of the type and size of the vessel in use, the operational water depth, environmental forces acting upon it, seabed (soil) conditions, and the competence of the mooring lines and anchors / clump weights.

These different factors must be closely complimentary for a mooring system to harness its full potential against environmental loads, which are predominant offshore. At a prototype scale, designing a mooring system for floating structures requires a careful consideration of all of these factors, keeping in mind the implications of the failure of the system. Understanding the behavior of the structure under operational loads is essential for a competent design. Considerations in the design must include the maximum permissible excursions of the vessel, proper choices for the mooring lines, anchors, and clump weights (if used); design life; cost; and failure modes such as the snapping of the mooring lines and fatigue damage. Of equal (if not greater) importance is the verification of the global analysis performed in the design of floating structures and their moorings. Conscious of the fact that such structures will be exposed to great environmental forces offshore, measures must be taken to ensure that their designs are appreciably reliable. One method of verifying the analysis performed in the prototype design process is model testing. A model of the designed floater is built and subjected to the same environmental loads in a wave basin as those used in the prototype design. During testing, the responses of the floater to the various forces caused by winds, waves, and currents are measured and compared to those obtained in the design of the prototype floater. As long as the testing procedure is conceptually and practically correct, the results obtained independently represent the performance to be expected of the prototype floater under the given loading conditions, if it is installed in the field. Therefore, the role of model testing in the verification of designs for floating structures is truly unique. Conducting model tests requires wave basins, which are typically limited in their depth and spatial dimensions. Although the model floater is typically much smaller than the prototype system, depending on the model scale chosen, a basin's dimensions may not be sufficiently large to accommodate the directly scaled mooring system. Consequently, the size of the floater and the accompanying mooring system are reduced to allow them to adequately fit into the test facility. The test engineer has the primary task of replicating the static behavior of the prototype system on the model to be tested in the wave basin. Essentially, the effects of the mooring system in the wave basin on the model floater must be equal to those that the prototype mooring system has on the full-depth floater. This introduces the need for equivalent mooring systems to represent the moorings of a full depth system. In many publications, the terms "equivalent mooring systems" and "truncated mooring systems" are used interchangeably. However, doing so defiles their individual definitions. In a later section of this report, a proper distinction between the two is drawn for clarity.

2. Components of Mooring System

The factors that determine the types of mooring lines and components to use in a prototype system include durability, compatibility with the global system, cost, and functionality under the environmental conditions in which they will be operating. The mooring lines considered for discussion include steel cable (or wire rope), chain, synthetic fiber (nylon and polyester) rope, and springs. Typically, these are the mooring line types deployed in the model testing of deepwater floating structures. Other mooring components include different types of anchors and connectors. Steel cables or wire ropes could be made out of carbon steel or stainless steel. They find extensive application in deepwater operations because of their high strength-to-size ratios.

Fig. 2.1: Stainless steel cable.

Chains are also used in statically equivalent mooring systems, and their unique characteristic is providing catenary effects in the mooring lines.

Fig. 2.2: Studless mooring chain.

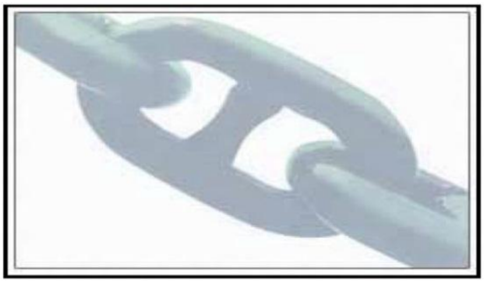

Fig. 2.3: Stud-linked mooring chain.

Synthetic fiber ropes are highly applicable in offshore mooring systems. These ropes essentially find greater applicability in deepwater over chains and wire ropes because they are much lighter in weight, and possess very good strengthto- submerged weight ratios.

Fig.2.4: Synthetic fiber rope.

Connectors or links such as shown in fig 2.5 could be components of an equivalent mooring system. Links enable a combination of different mooring line components having varying properties.

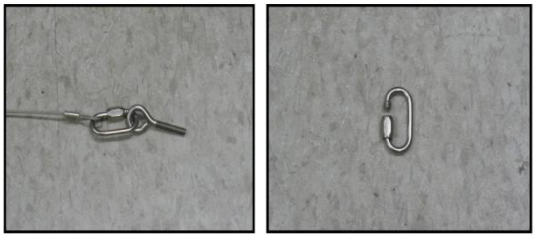

Fig. 2.5: Connectors for model scale mooring.

Fairleads are important components of mooring systems, and are provided to guide mooring lines around the floating structure. In some cases, the floater's hull could be built in such a way that the fairleads are holes within the hull, while in other cases they could be separate pieces of hardware attached to the vessel's hull. This research focuses on spread mooring systems only, which can be classified as shown in fig. 2.6.

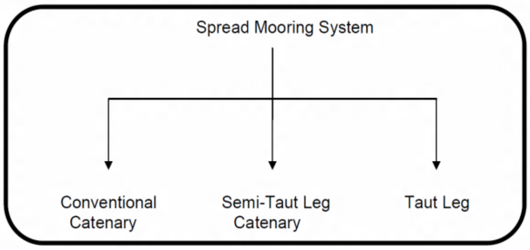

Fig. 2.6: Classification of spread mooring systems.

3. Design Related Limitation

In a study by Kim (2004) at the OTRC, the FPSO responses in hurricane seas predicted by a vessel-mooring-riser coupled dynamic analysis program were compared to wave tank measurements. A tanker-based turret-moored FPSO moored by 12 chain-polyester-chain taut lines in 6,000 ft of water was studied. A series of model tests (with a 1:60 scale) were conducted in the OTRC's wave basin at Texas A&M University with a statically-equivalent mooring system to assess its performance under hurricane conditions. The conclusions reached in this study include the facts that the differences between the measured and predicted results could can be attributed to the uncertainties related to viscous effects, wind force generation, the current profile and its unsteadiness, the mooring line truncation, and the use of springs, buoys, and clump weights in the equivalent mooring lines. It is believed that the numerical modeling of the equivalent mooring system would have been more feasible if the equivalent system was less complex (i.e., without clump weights, buoys, etc.); such a relatively simpler set-up could easily embrace the use of a fit-for-purpose software for the direct numerical modeling of a statically equivalent mooring system, thereby reducing the uncertainties related to mooring line truncation.

A review of the model testing procedures for the global analysis verification of floating production systems in ultra deepwaters is given in the work of Stansbeg, Karlsen, Ward, Wichers, and Irani (2004). Their work suggests guidelines to for this verification process, with the philosophy that a numerical model of the equivalent set-up is validated against the tests, and the resulting calibration information is then applied in full-depth verification simulations. The principles for designing equivalent systems are also discussed. The concerns expressed in their work include the challenges in model testing, the greatest of which is the spatial limitations of wave tanks. They recommend a hybrid method in which numerical models are used in the design of statically equivalent mooring systems and discuss a procedure based on guidelines worked out for DeepStar as a part of a more general guideline study on the global analysis of deepwater floating production systems (2004).

In an earlier study by Stansberg, Ormberg, and Oritsland (2002) on the challenges in deep water experiments, the use of a hybrid method to obviate some of the uncertainties in the design of statically equivalent mooring systems is explicitly presented. It is no surprise that the background information in this work is similar to that of Stansberg and others (2004). Fylling and Stansberg (2005) used a non – linear optimization code to reduce the manual iteration work in designing statically equivalent mooring systems. They explain explicitly that the hydrodynamic loads on a floating structure are not directly influenced by the mooring systems, and therefore tests with smaller water depths can be used to obtain the hydrodynamic characteristics of the floating structure.

Ormberg, Stansberg, and Yttervik (1999) worked on an integrated vessel motion and mooring analysis in hybrid model testing. Smith and MacFarlane (2001) present four methods to solve catenary equations for a three-component mooring system, made up of two line segments connected at a buoy or sinker. The different methods presented are peculiar to the specific configurations of the system. Their analysis assumes that the water depth and fairlead tensions are given.

Menezes and Martha (2005) present a steady-state genetic algorithm to solve mooring pattern optimization problems, owing to the fact that traditional optimization methods fail to efficiently provide reliable results. Mooring systems involving the use of chains show the major loading mechanisms to be twist (on the vessel attachment), bending (within the fairlead), high tensions (just below, or at the fairlead) fatigue (within the arc length of the line), and wear (toward the end of the line), as illustrated in fig. 3.1(2008).

Fig. 3.1, Loading mechanisms on offshore mooring chains:

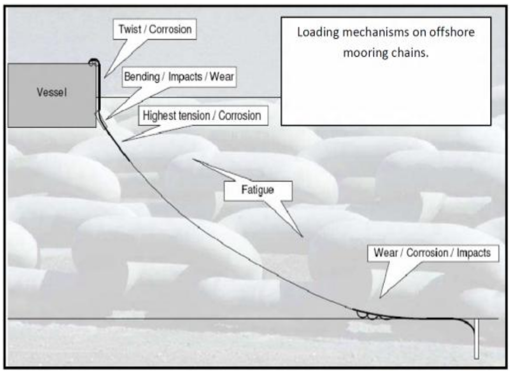

Fig. 3.1: Loading mechanisms on offshore mooring chains.

Like any other mooring line type used in offshore operations, chains experience a range of cyclic tension variations, which induce tension fatigue. Figure 3.2 shows examples of chain fatigue.

Fig. 3.2: Fatigued sections of mooring chain.

4. Formulation of Static Analysis

Given that a spread mooring system comprises several individual catenary mooring lines, the procedure used in the analysis of a single line forms the basis for resolving the static parameters of a spread mooring system. The fundamental principles of system equilibrium apply, and can be expressed in the following equations:

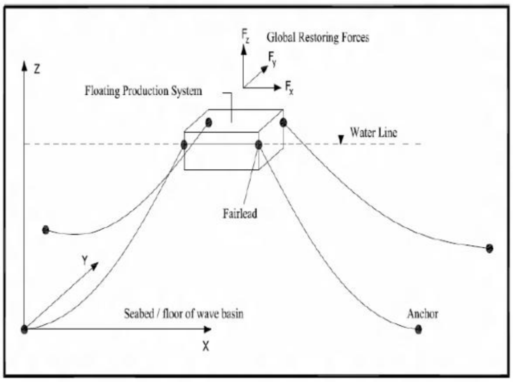

Fig. 4.1: Sketch of spread mooring system with 4 mooring lines in elevation.

$$\sum F_X = 0 \tag{4.1}$$

$$\sum F_Y = 0 \tag{4.2}$$

$$\sum F_Z = 0 \tag{4.3}$$

Considering fig. 4.1, eqns. (4.1) to (4.3) are the only equilibrium equations of interest regarding the static equivalence under discussion. Although an additional static equilibrium equation($\sum M_X = 0, \sum M_Y = 0, \sum M_Z = 0$) could be considered, the floater is assumed (at the moment) not to rotate. Hence, the moment equilibrium is not considered. The primary target is to ensure that the static global horizontal forces and stiffness on the floating vessel in the equivalent system are close enough to those of the prototype system.

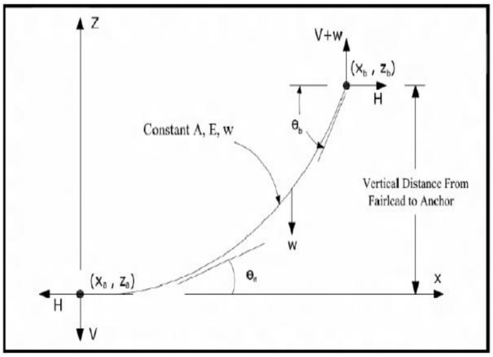

Fig. 4.2: Single-segment mooring.

For a single segment mooring under equilibrium conditions such as those shown in fig. 3.2, the equilibrium equations for a static analysis can be derived as shown in eqn. (4.4). The configuration in fig. 4.2 and the subsequently derived equations are specifically for the case where point "a" (the left end of the line) corresponds to the catenary touchdown point or to a point where there is a vertical uplift component to the tension. It is assumed that the water is calm, that is, it does not exert a force on the cable (other than buoyancy). The submerged unit weight of the cable is w (weight per unit length).

Considering an isolated elemental length, ds of the line in fig. 3.2, the free body diagram can be drawn as shown in fig 3.3. The tension, T, at the left end of the section is replaced by its vertical and horizontal components, V and H, respectively, and the submerged weight per unit length is w.

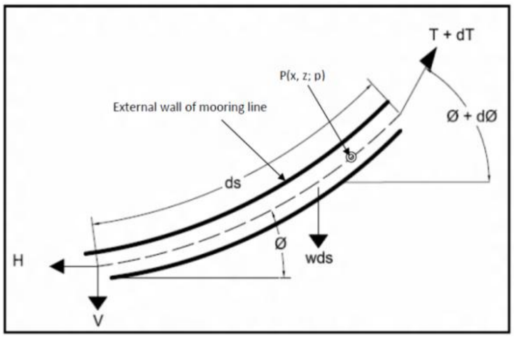

Fig. 4.3: Free body diagram of elemental section.

Taking the summation of the forces on the horizontal axis in fig. 4.3:

$$\sum F_X = 0$$

$$-H + (T + dT)\cos(\varphi + d\varphi) = 0 \tag{4.4}$$

Using the identity:
$\cos(\varphi + d\varphi) = \cos\varphi\cos d\varphi - \sin\varphi\sin d\varphi$
Equation (4.4) can be written as:
$-H + (T + dT).[\cos\varphi\cos d\varphi - \sin\varphi\sin d\varphi] = 0$
$-H + (T + dT)\cos\varphi\cos d\varphi - (T + dT)\sin\varphi\sin d\varphi = 0$
If we assume that $d\varphi$ is small, then
$\cos d\varphi \approx 1$ and $\sin d\varphi \approx d\varphi$
$-H + (T + dT)\cos\varphi - (T + dT)\sin\varphi d\varphi = 0$
$-H + T\cos\varphi + dT\cos\varphi - T\sin\varphi d\varphi - dT\sin\varphi d\varphi = 0$
Since $H = T\cos\varphi$,
$dT\cos\varphi - T\sin\varphi d\varphi - dT\sin\varphi d\varphi = 0$
We can consider the third term on the left hand side to be very small relative to the other terms; hence we neglect it to obtain:

$$dT\cos\varphi - T\sin\varphi d\varphi = 0 \tag{4.5}$$

from which:

$$\frac{dT}{T} = \tan\varphi d\varphi \tag{4.6}$$

Similarly, we take the summation of the forces on the vertical axis in fig. 4.3:

$$\sum F_z = 0$$

$$-V - wds + (T + dT)\sin(\varphi + d\varphi) = 0 \tag{4.7}$$

$-V - wds + (T + dT).[\cos\varphi\cos d\varphi - \sin\varphi\sin d\varphi] = 0$

Again if we assume that $d\varphi$ is small, then
$\cos d\varphi \approx 1$ and $\sin d\varphi \approx d\varphi$

$$T\cos\varphi d\varphi + dT\sin\varphi = wds \tag{4.8}$$

Substituting eqn. (4.6) into eqn. (4.8)

$T(\cos\varphi d\varphi + \tan\varphi d\varphi\sin\varphi) = wds$

If we substitute

$T = \frac{H}{\cos\varphi}$ and $\tan^2\varphi = \sec^2\varphi - 1$

we obtain:

$$\frac{H}{\cos^2\varphi}d\varphi = wds$$

Integrating both sides, we have:

$$H\int\frac{1}{\cos^2\varphi}d\varphi = w\int ds$$

$$\frac{w}{H}s = \tan\varphi + C \tag{4.9}$$

At s=0, $\varphi = \varphi_a$ and therefore $C = -\tan\varphi_a$

Therefore eqn. (4.9) can be written as:

$$ws = H\tan\varphi - H\tan\varphi_a \tag{4.10}$$

which can also be written as:

$$V = ws + H\tan\varphi_a \tag{4.11}$$

The magnitude of the tension in the mooring line at point “a” can be expressed as:

$T = \sqrt{H^2 + V^2}$

Therefore, along the mooring line, the tension as a function of the arc length can be expressed in terms of eqn. (4.11) as:

$$T(s) = \sqrt{H^2 + (ws + H\tan\varphi_a)^2} \tag{4.12}$$

Or

$$T(s) = H\sqrt{1 + (\frac{ws}{H} + \tan\varphi_a)^2} \tag{4.13}$$

Equation (4.12) or (4.13) gives the tension distribution along the mooring line. As in Irvine (2001), let s be the Lagrangian coordinate of the unstretched mooring line. We can define a point, P, along this s coordinate. However, under the self weight of the line (or external loads) point P moves to occupy a new position in the stretched configuration of the mooring line, as described by Cartesian coordinates x, and z and Lagrangian coordinate p. With respect to point P we can write:

$$\cos\varphi = \frac{dx}{dp} \tag{4.14}$$

And

$$\sin\varphi = \frac{dz}{dp} \tag{4.15}$$

Thus, we can write the horizontal component of the tension at point P as:

$$H = T\frac{dx}{dp} \tag{4.16}$$

It is assumed that the elasticity of the mooring line can be modeled by Hooke's law as:

$$\frac{\Delta L}{L_0} = \frac{T}{EA_0} \tag{4.17}$$

where L_0 is the un-stretched length of the line (under no tension), E is the Young's modulus of the mooring line, and A_0 is the effective cross-sectional area of the mooring line. The ratio of the change in length to the original length can also be expressed as:

$$\frac{\Delta L}{L_0} = \frac{dp}{ds} - \frac{ds}{ds} = \frac{dp}{ds} - 1 \tag{4.18}$$

So, from eqns. (4.17) and (4.18),

$$T = \left(\frac{dp}{ds} - 1\right)EA_0$$

$$\frac{dp}{ds} = \frac{T}{EA_0} + 1 \tag{4.19}$$

The change along the x coordinate with respect to the Lagrangian coordinate, s,can be expressed as:

$$\frac{dx}{ds} = \frac{dx}{dp}.\frac{dp}{ds} \tag{4.20}$$

From eqn. (3.16):

$$\frac{dx}{dp} = \frac{H}{T} \tag{4.21}$$

Therefore, substituting eqns. (4.19) and (4.21) into (4.20), we have:

$$\frac{dx}{ds} = \frac{H}{T}\left(\frac{T}{EA_0} + 1\right) = \frac{H}{EA_0} + \frac{H}{T} \tag{4.22}$$

Substituting eqn. (4.12) in eqn. (4.22), we have:

$$dx = \frac{H}{EA_0}ds + \frac{H}{\sqrt{H^2+(ws+V)^2}}ds \tag{4.23}$$

Recalling that the integral of the form

$$\int \frac{1}{\sqrt{a^2+x^2}}dx = \sinh^{-1}(\frac{x}{a})$$

On integration, eqn. (4.23) becomes:

$$x(s) = \frac{Hs}{EA_0} + H\left\{\frac{1}{w}(\sinh^{-1}\left(\frac{ws+V}{H}\right))\right\} + C \tag{4.24}$$

At s = 0, x(0) = 0 , so

$$C = \frac{-H}{w}\left\{\sinh^{-1}\left(\frac{V}{H}\right)\right\}$$

and therefore

$$x(s) = \frac{Hs}{EA_0} + \frac{H}{w}\left\{\sinh^{-1}\left(\frac{ws+V}{H}\right) - \sinh^{-1}\left(\frac{V}{H}\right)\right\} \tag{4.25a}$$

Equation (4.25a) gives the x coordinate of the mooring line as a function of s . For an inextensible mooring line, $EA_0 \rightarrow \infty$, and eqn. (4.25a) reduces to (3.25b):

$$x(s) = \frac{H}{w}\left\{\sinh^{-1}\left(\frac{ws+V}{H}\right) - \sinh^{-1}\left(\frac{V}{H}\right)\right\} \tag{4.25b}$$

Similar to eqn. (4.20), with respect to the z axis:

$$\frac{dz}{ds} = \frac{dz}{dp}.\frac{dp}{ds} \tag{4.26}$$

Recall from eqn. (4.19) that: $\frac{dp}{ds} = \frac{T}{EA_0} + 1$

From eqn. (3.15):

$$\sin\varphi = \frac{dz}{dp} = \frac{V}{T}$$

Substituting into eqn. (4.26)

$$dz = \frac{V}{EA_0}ds + \frac{V}{T}ds \tag{4.27}$$

Now with respect to eqn. (4.11), we can write eqn. (4.27) as:

$$dz = \frac{ws + H\tan\varphi_a}{EA_0}ds + \frac{ws + H\tan\varphi_a}{\sqrt{H^2+(ws+V)^2}}ds \tag{4.28}$$

The integration of eqn. (3.28), where the second term is integrated by the substitution method, yields:

$$z(s) = \frac{ws^2}{2EA_0} + \frac{Hs\tan\varphi_a}{EA_0} + \frac{H}{w}[1 + (\frac{ws}{H} + \tan\varphi_a)^2]^{1/2} + C \tag{4.29}$$

At s = 0, z(0) = 0 , so

$$\frac{H}{w}[1 + \tan{\varphi_a}^2]^{1/2} + C = 0$$

Therefore

$$C = -\frac{H}{w}\sec\varphi_a$$

Equation (4.29) can now be written as:

$$z(s) = \frac{ws^2}{2EA_0} + \frac{Hs\tan\varphi_a}{EA_0} + \frac{H}{w}[1 + (\frac{ws}{H} + \tan\varphi_a)^2]^{1/2} - \frac{H}{w}\sec\varphi_a \tag{4.30}$$

Therefore the z coordinate of the mooring line as a function of s is given by eqn. (4.30). For an inextensible mooring line, $EA_0 \rightarrow \infty$, and eqn. (4.30) reduces to:

$$z(s) = \frac{H}{w}\left\{[1 + (\frac{ws}{H} + \tan\varphi_a)^2]^{1/2} - \sec\varphi_a\right\} \tag{4.31}$$

We can derive an expression for the arc length s of the mooring line as a function of the x coordinate, using the governing differential equation of the catenary. Recalling eqn. (4.10):

$$ws = H\tan\varphi - H\tan\varphi_a$$

$$\frac{ws}{H} = \frac{dz}{dx} - \tan\varphi_a \tag{4.32}$$

Differentiating both sides with respect to x :

$$\frac{d}{dx}(\frac{ws}{H}) = \frac{d^2z}{d^2x} \tag{4.33}$$

Equation (4.33) is the governing differential equation of the catenary line.
Since
$(ds)^2 = (dx)^2 + (dz)^2$, we can write

$$\frac{ds}{dx} = [1 + z'^2]^{1/2} \tag{4.34}$$

Where $z' = \frac{dz}{dx}$ (4.35)

Substituting eqn. (4.34) into eqn. (4.33),

$$H\frac{d^2z}{d^2x} = w[1 + z'^2]^{1/2}$$

$$\frac{w}{H} = \frac{\frac{d^2z}{d^2x}}{[1 + z'^2]^{1/2}}$$

$$\int \frac{w}{H}dx = \int \frac{1}{[1 + z'^2]^{1/2}}dz'$$

$$\frac{w}{H}x = \sinh^{-1}z' + C_1$$

$$z' = \sinh(\frac{w}{H}x - C_1)$$

$$z = \int \sinh\left(\frac{w}{H}x - C_1\right) = \frac{H}{w}\cosh\left(\frac{w}{H}x - C_1\right) + C_2$$

At x=0, $z' = \tan\varphi_a$, therefore

$$C_1 = -\sinh^{-1}(\tan\varphi_a)$$

At x = 0, z = 0, therefore

$$C_2 = -\frac{H}{w}\cosh(\sinh^{-1}(\tan\varphi_a))$$

Therefore;

$$z(x) = \frac{H}{w}[\cosh\left(\left(\frac{w}{H}x + \sinh^{-1}(\tan\varphi_a)\right)\right. - \cosh\left(\sinh^{-1}(\tan\varphi_a)\right)] \tag{4.36}$$

Equation (4.36) gives the vertical coordinate of a mooring line as a function of x , the horizontal coordinate. From equation (4.32);

$$s(x) = \frac{H}{w}\left(\frac{dz}{dx} - \tan\varphi_a\right) = \frac{H}{w}\left\{\sinh\left[\frac{wx}{H} + \sinh^{-1}(\tan\varphi_a)\right] - \tan\varphi_a\right\} \tag{4.37}$$

Equation 4.37 gives the arc length of the mooring line as a function of the horizontal coordinate, x. Other equations such as those for s(x) and z(x) may also be used in determining the static equilibrium, but this will depend on the numerical strategy adopted for the iteration process. To obtain static solutions using the equations, information must be provided:

1. The elevation of the top end of the mooring line segment, relative to the bottom end;
2. The line weight per unit length w, line length L, axial stiffness EA_0.
3. The horizontal component of the tension in the line (H), or the known horizontal offset position of the top end of the line relative to the bottom end.

The primary condition that must be satisfied (as applied in this research) to obtain correct static equilibrium solutions is that the computed vertical coordinate of the top attachment point of the line, z(s), must be close enough (or equal) to the specified fairlead elevation relative to the anchor point. It may be possible to control the numerical iteration using some other known constant parameter, but the condition stated above is the only one used in this work at this point.

5. Conclusions

The use of a hybrid method of design verification to verify the designs of deepwater floating structures is greatly embraced by the industry. As exposed in the discussed literature in the second step of this work, the processes of creating the model and designing a statically equivalent mooring system require efficient numerical tools. This research has provided a tool that is specifically tailored to perform one of the tasks required in the hybrid method.

Acknowledgment

This work was supported by a grant from Human Resources Development of the Korea Institute of Energy Technology Evaluation and Planning(KETEP), funded by the Korea government Ministry of Knowledge Economy (No. 20114030200070).

References

[1] Stansberg, C. T., Karlsen, S. I., Ward, E. G., Wichers, J. E. W. and Irani, M. B., (2004), "Model Testing for Ultradeep Waters," OTC Conference, Houston, OTC 16587, pp. 1 - 8.

[2] Fernandez, J., (2008), "Reliability of Mooring Chains," Proceedings of TEKNA Conference on DP and Mooring of Floating Offshore Units, Alesund, Norway.

[3] Kim, M. H., (2004), "Dynamic Analysis Tool for Moored Tanker-Based FPSO's Including Large Yaw Motions," Final Report Prepared for the Minerals Management Service under the MMS/OTRC Cooperate Research Agreement, http://www.mms.gov, pp. 2 - 4. 147.

[4] Luo, Y., Baudic, S., Poranski, P., Ormberg, H., Stansberg, C. T. and Wichers, J., (2004), "Prediction of FPSO Responses: Model Tests versus Numerical Analysis," OTC Conference, Houston, OTC 16585, pp. 1 - 7.

[5] Stansberg, C. T., Ormberg, H. and Oritsland, O., (2002), "Challenges in Deep Water Experiments: Hybrid Approach," Transactions of the ASME, 124, pp. 90 - 95.

[6] Fylling, I. J. and Stansberg, C. T., (2005), "Model Testing of Deepwater Floating Production Systems: Strategy for Truncation of Moorings and Risers," Proceedings of 17th DOT Conference, Vitoria, Brazil, pp. 1 - 4.

[7] Ormberg, H., Stansberg, C. T., Yttervik, R. and Kleiven, G., (1999),"Integrated Vessel Motion and Mooring Analysis Applied in Hybrid Model Testing," Proceedings of the 9th ISOPE Conference, Brest, France, I, pp. 339 - 346.

[8] Smith R. J. and MacFarlane, C. J., (2001), "Statics of a Three Component Mooring Line," Ocean Engineering, 28(7), pp. 899 – 914.

[9] Carbono, A. J., Menezes, I. F. M. and Martha, L. F., 2005, "Mooring Pattern Optimization using Genetic Algorithms," 6th World Congress of Structural and Multidisciplinary Optimization, Rio de Janeiro, Brazil, pp. 1 - 9.

[10] Irvine, H. M., 1981, "Cable Structures," MIT Press, Cambridge, MA, pp. 1- 24.